Cancer-associated epithelial cell adhesion molecule (EpCAM; CD326) enables epidermal Langerhans cell motility and migration in vivo

Maria R. Gaiser[a], Tim Lämmermann[b], Xu Feng[a], Botond Z. Igyarto[c], Daniel H. Kaplan[c], Lino Tessarollo[d], Ronald N. Germain[b], and Mark C. Udey[a,1]

[a]Dermatology Branch, Center for Cancer Research, National Cancer Institute, National Institutes of Health, Bethesda, MD 20892; [b]Lymphocyte Biology Section, Laboratory of Systems Biology, National Institute of Allergy and Infectious Diseases, National Institutes of Health, Bethesda, MD 20892; [c]Department of Dermatology, Center for Immunology, University of Minnesota, Minneapolis, MN 55455; and [d]Mouse Cancer Genetics Program, Center for Cancer Research, National Cancer Institute-Frederick, National Institutes of Health, Frederick, MD 21702

Edited* by Thomas A. Waldmann, National Cancer Institute, National Institutes of Health, Bethesda, MD, and approved February 8, 2012 (received for review October 26, 2011)

After activation, Langerhans cells (LC), a distinct subpopulation of epidermis-resident dendritic cells, migrate from skin to lymph nodes where they regulate the magnitude and quality of immune responses initiated by epicutaneously applied antigens. Modulation of LC–keratinocyte adhesion is likely to be central to regulation of LC migration. LC express high levels of epithelial cell adhesion molecule (EpCAM; CD326), a cell-surface protein that is characteristic of some epithelia and many carcinomas and that has been implicated in intercellular adhesion and metastasis. To gain insight into EpCAM function in a physiologic context in vivo, we generated conditional knockout mice with EpCAM-deficient LC and characterized them. Epidermis from these mice contained increased numbers of LC with normal levels of MHC and costimulatory molecules and T-cell–stimulatory activity in vitro. Migration of EpCAM-deficient LC from skin explants was inhibited, but chemotaxis of dissociated LC was not. Correspondingly, the ability of contact allergen-stimulated, EpCAM-deficient LC to exit epidermis in vivo was delayed, and strikingly fewer hapten-bearing LC subsequently accumulated in lymph nodes. Attenuated migration of EpCAM-deficient LC resulted in enhanced contact hypersensitivity responses as previously described in LC-deficient mice. Intravital microscopy revealed reduced translocation and dendrite motility in EpCAM-deficient LC in vivo in contact allergen-treated mice. These results conclusively link EpCAM expression to LC motility/migration and LC migration to immune regulation. EpCAM appears to promote LC migration from epidermis by decreasing LC–keratinocyte adhesion and may modulate intercellular adhesion and cell movement within in epithelia during development and carcinogenesis in an analogous fashion.

Epidermal Langerhans cells (LC) are unique dendritic cells (DC) that are found in stratified squamous epithelia, including skin. Features that distinguish LC from other DC include morphologically distinct endocytic vesicles (termed "Birbeck granules") (1), an absolute dependence on TGF-β1 for development (2), relative radio-resistance that reflects a life span of months to years (3), and selective expression of several cell-surface proteins that are anticipated to have important functions. These proteins include Langerin (a C-type lectin) (4), E-cadherin (an intercellular adhesion molecule) (5), and epithelial cell adhesion molecule (EpCAM; CD326) (6) or its homolog TROP2 (TACSDT2) (7) in mice and humans, respectively. LC intercalate among keratinocytes (KC), and this intimate relationship is maintained as epithelial cells proliferate, differentiate, and are shed. Although resting LC are relatively sessile, they regularly extend and retract processes (dendrites) between KC, an activity termed "dendrite surveillance extension and retraction cycling habitude" (dSEARCH) (8) without disrupting epidermal integrity. LC movement within and emigration from epidermis is increased after LC activation, as is dSEARCH activity. Vertical projections of resting LC dendrites appear to be delimited by epidermal tight junctions that form in the immediate subgranular layer of the epidermis, whereas dendrites of activated LC can penetrate tight junctions, facilitating uptake of antigens that are present on skin surfaces (9).

Until recently, it was thought that LC were essential for initiation and propagation of effector T-cell responses directed toward antigens that breached the outermost epidermal barrier (the stratum corneum). Studies in mice that exhibit LC deficiencies have changed this paradigm. Recent studies indicate that LC do not function as essential antigen-presenting cells in contact hypersensitivity reactions (10–12) or antiviral responses (13, 14). Based on studies of contact hypersensitity (11, 15) and cutaneous leishmaniasis (16), an immune-attenuating role for LC has been suggested. However, additional studies suggest that LC do promote the T-helper (Th) cell-selective effector responses [e.g., Th2-predominant Ab responses after gene gun immunization (17) and Th17 responses to fungus-associated antigens that are encountered in skin (18)].

Functions of LC are predicated on the ability of LC to localize and persist in epidermis and to traffic from skin to lymph nodes (LN) in a carefully controlled fashion at baseline and after activation. Modulation of adhesion of LC to KC is likely to be central to the regulation of LC trafficking, and mechanistic details regarding LC-KC adhesion remain to be elucidated. We previously demonstrated that LC express E-cadherin (5), a homophilic adhesion molecule that is an important component of adherens junctions (19). It seems likely that LC trafficking is influenced by changes in E-cadherin–dependent LC–KC adhesion (20–22), but this concept has not been demonstrated formally.

EpCAM is another cell-surface protein that is expressed by LC (6) and that might regulate LC trafficking. This transmembrane glycoprotein is expressed in many developing epithelia (17, 23) and in some epithelia (e.g., intestinal epithelia) in adult animals (24). It has been suggested that EpCAM can promote intercellular adhesion through homophilic interactions (25) but also can attenuate cadherin-mediated adhesion (26). EpCAM also has been studied intensively in the context of cancer, both because, as a tumor antigen, it may represent a suitable target for

Author contributions: M.R.G., T.L., and M.C.U. designed research; M.R.G., T.L., X.F., and L.T. performed research; T.L., B.Z.I., D.H.K., and R.N.G. contributed new reagents/analytic tools; M.R.G., T.L., R.N.G., and M.C.U. analyzed data; and M.R.G., T.L., R.N.G., and M.C.U. wrote the paper.

The authors declare no conflict of interest.

*This Direct Submission article had a prearranged editor.

[1]To whom corrrespondence should be addressed. E-mail: udey@helix.nih.gov.

See Author Summary on page 5563 (volume 109, number 15).

This article contains supporting information online at www.pnas.org/lookup/suppl/doi:10.1073/pnas.1117674109/-/DCSupplemental.

immunotherapy (27) and because it may play a role in cancer pathogenesis (28). EpCAM expression correlates with tumor aggressiveness and poor prognosis and is linked to enhanced cancer cell migration, invasion, and metastasis (29). More recent studies have described a role for EpCAM in normal and cancer stem function (30) and also suggested that EpCAM may be an outside–in signaling molecule (31) that acts via a mechanism that involves sequential proteolysis of EpCAM that is coupled to regulation of transcription (31).

Most of what is known about EpCAM function is based on studies of clonal transformed cells, and many reports emphasize in vitro experiments. Conclusions drawn from such studies may or may not be relevant to normal physiology (relating to LC or other cells) or pathologic processes (such as cancer initiation and progression) as they evolve in vivo. To begin to relate EpCAM expression to LC function, several years ago we generated EpCAM KO mice (32) using preexisting ES cells that carried a targeted *EpCAM* allele that had been generated by gene trapping (33). Although heterozygous $EpCAM^{-/-}$ mice did not exhibit abnormalities, intercrossing these individuals failed to yield viable $EpCAM^{-/-}$ animals because $EpCAM^{-/-}$ embryos became nonviable at approximately embryonic day 12 secondary to placental insufficiency (32). This mortality precluded studies of LC and other lineages in postnatal EpCAM KO mice.

To circumvent the embryonic lethality associated with homozygous *EpCAM*-null mutations, we engineered mice with floxed *EpCAM* alleles that could be inactivated by introducing *Cre* recombinase using a transgenic approach. Here we describe conditional deletion of *EpCAM* in adult mice. For this initial study, we generated mice with EpCAM-deficient LC and determined that EpCAM that is expressed by LC regulates LC–KC interactions and LC trafficking. These results increase our understanding of the significance of EpCAM expression by LC, reiterate the importance of LC trafficking in LC function, and also may relate to EpCAM function in normal epithelia and cancer cells.

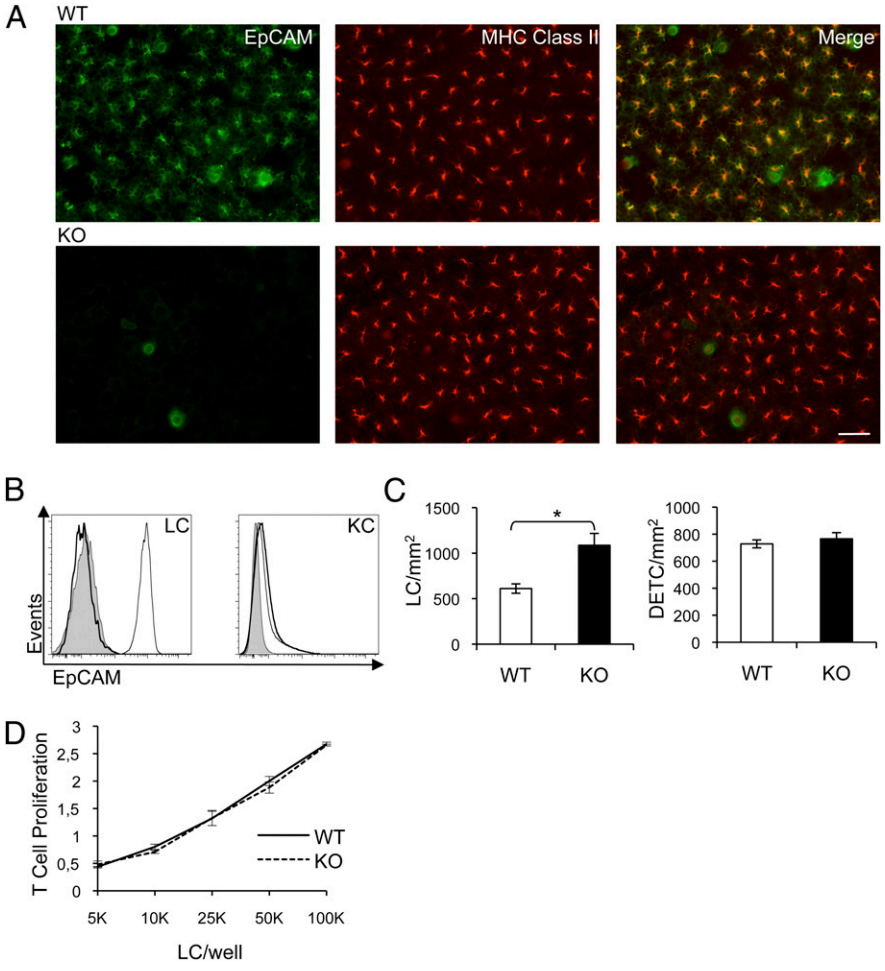

Fig. 1. Characterization of EpCAM-deficient LC in LC/EpCAM-cKO mice. (*A*) Demonstration in situ via immunofluorescence microscopy of EpCAM deletion in LC in LC/EpCAM-cKO mice. Epidermal sheets from LC/EpCAM-cKO (KO) and *Cre*-negative (WT) animals were stained with anti-EpCAM and anti-MHC Class II mAb and visualized using immunofluorescence microscopy (Scale bar: 50 μm.) Note residual EpCAM expression in hair follicles in WT and KO mice. (*B*) Demonstration via flow cytometry of EpCAM deletion in LC in LC/EpCAM-cKO mice. Flow cytometric analysis of $CD45^+$ MHC Class II^+ $Langerin^+$ cells (LC) and $CD45^-$ MHC Class II^- cells (KC) in epidermal cell suspensions from LC/EpCAM-cKO (KO) and WT animals. $n = 3$ mice per group in three experiments; thick line, KO; thin line, WT; gray line with shading, isotype control. EpCAM expression levels are depicted as geometric mean fluorescence intensities (MFI). (*C*) Increases in LC densities in LC/EpCAM-cKO mice. LC were enumerated by counting MHC Class II^+ cells in epidermal sheets from KO and WT mice (five random fields per mouse; $n = 5$ mice per group in six experiments.) $^*P < 0.005$. DETC (TCR γ/δ-positive cells) were quantified in epidermal sheets from KO and WT mice (five random fields per mouse, $n = 3$ mice per group in a single experiment). (*D*) T-cell–stimulatory activity of EpCAM-deficient LC. Epidermal cells from KO and WT mice were cocultured with MHC-mismatched (BALB/c) naive T cells ($n = 3$ mice per group in three experiments using triplicate measurements in each experiment). Numbers of LC per well were determined using flow cytometry to assess LC frequency in epidermal single-cell suspensions. T-cell proliferation was measured by quantifying cleavage of WST-1 using a spectrophotometric assay.

Results

Generation and Characterization of Mice with EpCAM-Deficient LC. We engineered mice with a floxed *EpCAM* allele that could be conditionally inactivated (EpCAM-cKO mice) using recombineering methodology (Fig. S1) (34). *LoxP* sites were inserted upstream and downstream of exons 1 and 2 of *EpCAM* in ES cells using a targeting vector that contained a neomycin-resistance gene flanked by *FRT* sites (Fig. S1*A*). Chimeric mice were generated using selected ES cells, germline transmission of the targeted allele was established, and the neomycin-resistance marker was deleted by crossing these mice with transgenic mice expressing *Flp* recombinase under control of the phosphoglycerate kinase 1 promoter [Flp deleter mice (35)] (Fig. S1 *A–C*). The mice that resulted ($EpCAM^{fl/fl}$ or EpCAM-cKO mice) were indistinguishable from unmanipulated mice. Importantly, insertion of *loxP* sites into the *EpCAM* locus did not influence expression of EpCAM by LC or KC obtained from EpCAM-cKO mice (Fig. S1*D*).

EpCAM-cKO mice subsequently were crossed with huLangerinCre^{tg+} mice that selectively express *Cre* recombinase in epidermal LC (11) to generate mice with EpCAM-deficient LC in an otherwise WT background (LC/EpCAM-cKO mice) (see Fig. S1*A* for a schematic representation of the anticipated recombined *EpCAM* gene). Immunofluorescence staining of epidermal sheets from WT and LC/EpCAM-cKO mice demonstrated virtually complete deletion of EpCAM in MHC Class II^+ epidermal cells (LC) in LC/EpCAM-cKO animals with persistent low-level expression of EpCAM by some follicular KC (Fig. 1*A*). Flow cytometric assessment of epidermal cell suspensions confirmed the in situ staining results (Fig. 1*B*). Deletion of EpCAM in LC did not result in cutaneous abnormalities that were evident by inspection or by routine histology of trunk (Fig. S1*E*, *Upper*) or ear (Fig. S1*E*, *Lower*) skin. Lineage-selective deletion of EpCAM was confirmed by assessing EpCAM expression in intestine. Immunofluorescence staining of frozen sections of small intestine revealed high levels of EpCAM on intestinal epithelial cells in both LC/EpCAM-cKO and WT mice, as expected (Fig. S1*F*).

Phenotypic and Functional Characterization of EpCAM-Deficient LC. Immunofluorescence images suggested that LC frequencies were higher in LC/EpCAM-cKO epidermis than in controls. Enumeration of LC in epidermal sheets revealed that LC were approximately twofold more frequent in KO mice than in WT mice, whereas dendritic epidermal T cells were represented similarly in both strains (Fig. 1*C*). Flow cytometric studies of $CD45^+$ MHC Class II^+ LC from unperturbed epidermis or from ear skin that had been treated with 1% 2,4,6-trinitrochlorobenzene (TNCB) 18 h previously did not reveal differences between EpCAM-deficient and control LC in the expression of MHC Class II, CD86, CD40, or E-cadherin (Fig. S2*A*). Both EpCAM-deficient and WT LC also up-regulated MHC Class II and costimulatory molecules to similar extents during a 72-h culture period (Fig. S2*B*), and the ability of WT and KO LC to stimulate proliferation of naive allogeneic CD4 T cells was indistinguishable (Fig. 1*D*). These results indicate that EpCAM is not required for LC development or homing, LC activation or maturation, or LC accessory cell activity as assessed by stimulation of naive T cells in vitro.

EpCAM Is Required for Efficient Emigration of LC from Skin Explants. The ability of LC to traffic from epidermis to regional LN is thought to be critical for LC function. In addition, both in vitro and in vivo studies previously have implicated EpCAM in intercellular adhesion and/or migration (23, 26, 36). These data, together with the increased numbers of steady-state LC in the skin of LC/EpCAM-cKO mice, suggested that EpCAM might regulate LC migration, an idea that we tested in vitro and in vivo. Flotation of mouse ear skin explants on medium including the chemokine CCL21 for 72 h revealed retention of EpCAM-deficient MHC Class II^+ $Langerin^+$ LC in epidermis as compared with WT LC, with a corresponding decrease in the accumulation of EpCAM-deficient MHC Class II^+ $Langerin^+$ LC in cords (representing lymphatics) (37, 38) in the dermis of explants (Fig. 2*A*). Enumeration of MHC Class II^+ $Langerin^+$ $CD103^-$ LC that accumulated in the medium containing explants during a 72-h incubation revealed an approximately twofold decrease in wells containing LC/EpCAM-cKO as compared with wells containing WT skin (Fig. 2*B*). Fewer Langerin-expressing dermal DC (dDC) (MHC Class II^+ $Langerin^+$ $CD103^+$cells) than LC emigrated from explants from mice of both genotypes, and EpCAM expression did not influence $Langerin^+$ dDC migration. LC that migrated from WT and LC/EpCAM-cKO explants expressed identical levels of the maturation markers MHC Class II, CD86, and CD40 (Fig. S2*C*).

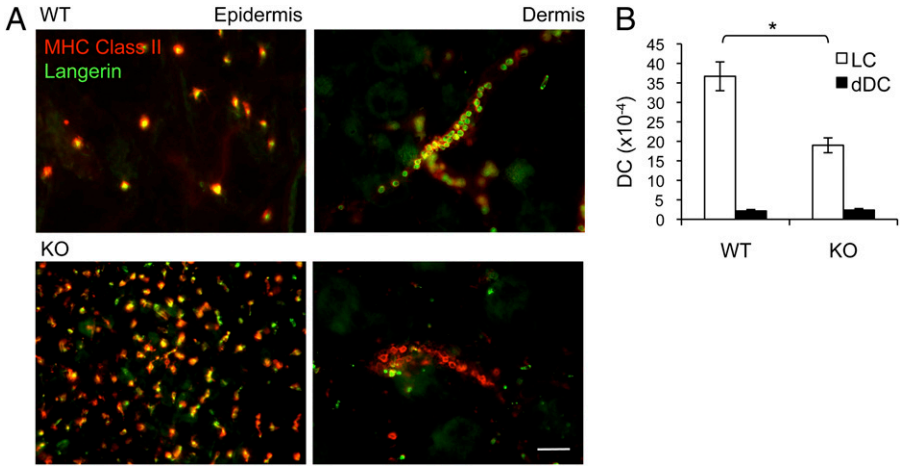

Fig. 2. Identification of a LC migration defect in skin explants from LC/EpCAM-cKO mice. (*A*) Retention of EpCAM-deficient LC in epidermis and paucity of EpCAM-deficient LC in the dermis of explants. Epidermal and dermal sheets were prepared from ear skin from LC/EpCAM-cKO (KO) and WT animals after flotation for 72 h on medium containing CCL21 (0.1 μg/mL) using ammonium thyiocyanate, stained with anti-Langerin and anti-MHC Class II mAb, and visualized using immunofluorescence microscopy. (Scale bar: 50 μm.) (*B*) Selective decreases in the migration of EpCAM-deficient LC from skin explants. Ear skin from KO and WT animals was floated on medium including CCL21 (0.1 μg/mL), and emigrated cells were counted after 72 h. White bars represent LC (MHC Class II^+ $Langerin^+$, $CD103^-$ cells); black bars represent dDC (MHC Class II^+, $Langerin^+$, $CD103^+$ cells). Data are from five experiments. $n = 5$ mice per group. $^*P < 0.001$.

To exclude a global requirement for EpCAM in LC motility or chemokine-induced LC migration, we assessed the ability of cultured LC to migrate in a 3D, dermis-like environment comprised of type I collagen toward a cytokine gradient in vitro in real time (ref. 39 and *Materials and Methods*). In the absence of CCL19, neither EpCAM-deficient nor control LC exhibited significant directional migration over the 3-h observation period. Introduction of chemokine induced migration of both LC/EpCAM-cKO and WT LC. The directionalities and velocities of chemokine-induced migration of EpCAM-deficient and control LC could not be distinguished (Fig. 3 *A* and *B* and Movie S1), indicating that EpCAM is not required for interstitial migration of isolated LC in vitro.

Involvement of EpCAM in LC Migration in Vivo. To assess the in vivo relevance of our in vitro findings, we studied the behavior of LC in contact allergen-treated LC/EpCAM-cKO mice. Treatment of WT and LC/EpCAM-cKO ear skin with 1% TNCB led to activation of significant subpopulations of LC (manifested by increased MHC Class II and CD86 expression over baseline) 36 h after TNCB treatment, as anticipated (Fig. 4*A*). In initial experiments, the frequency of activated LC appeared to be higher in LC/EpCAM-cKO mice than in WT mice 36 h after TNCB exposure. Extension of these studies revealed that similar proportions of activated LC (approximately 25%) were detected in TNCB-treated KO and WT skin 18 h after hapten application (Fig. 4*B* and Fig. S3). At the 36-h time point [and after emigration of activated LC from TNCB-treated epidermis had begun (20)], the number of activated LC was approximataely twofold higher in LC/EpCAM-cKO epidermis than in WT epidermis. Differences between the number of activated LC in hapten-treated KO and WT epidermis were not evident by 48 h after TNCB treatment. These results suggest that EpCAM-deficient LC are activated efficiently after application of TNCB to skin, but their ability to exit epidermis after activation is attenuated.

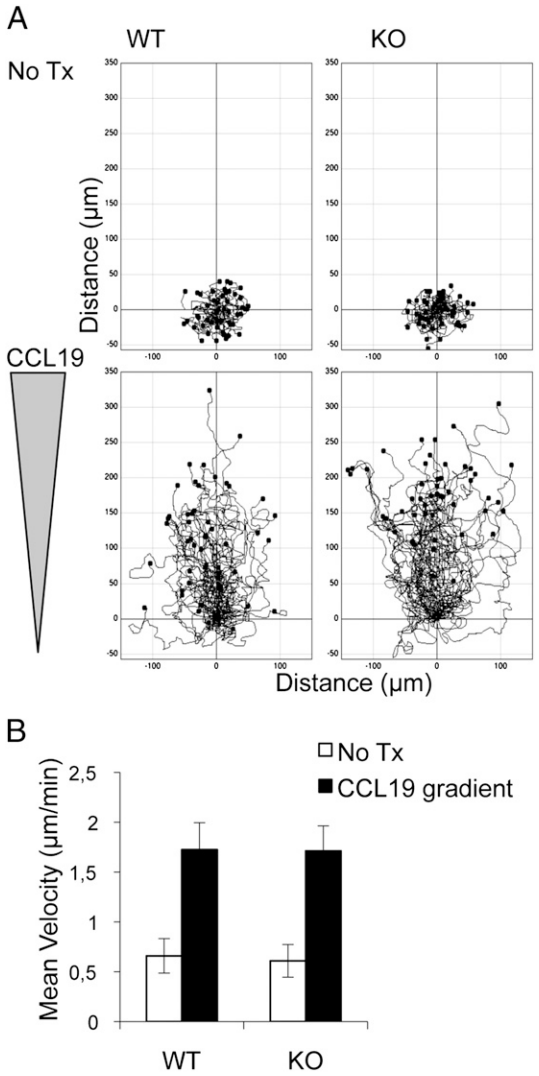

Fig. 3. Normal chemotaxis of EpCAM-deficient LC in collagen gels. (*A*) Representative tracks of single LC migrating toward CCL19 within type I collagen networks. Fifty LC of each genotype were tracked, and individual tracks are displayed in a 2D graphic. The intersection of horizontal and vertical lines represents the originating location for each cell at the beginning of the observation period. (*B*) Quantification of LC chemotaxis in vitro. Velocities of WT and EpCAM-deficient LC migrating toward CCL19 in collagen gels. Migration was measured over 3 h at 1-min intervals using 10× magnification (10 cells per field were tracked, five fields per group). Data depicted represent mean velocities ± SEM of three experiments. No TX, no treatment.

We predicted that inhibition of the ability of EpCAM-deficient LC to emigrate from contact allergen-treated epidermis would result in delayed or reduced accumulation of hapten-bearing cells in skin-draining LN. To test this hypothesis, we enumerated LC in inguinal and axillary LN of WT and LC/EpCAM-cKO mice before and after treatment of skin with TRITC in acetone:dibutyl phthalate. Flow cytometry of skin-draining LN cells obtained 96 h after TRITC painting revealed fewer $TRITC^+$ $CD11c^+$ MHC Class II^{hi} DC in the LN of KO mice (5%) than in WT mice (18%) (Fig. 4*C*). Enumeration of $TRITC^+$ $CD11c^+$ MHC $ClassII^{hi}$ $Langerin^+$ $CD103^-$ $CD11b^+$ cells in WT mice at various times after TRITC treatment indicated that, as expected (12), numbers of hapten-bearing LC that accumulated in LN were maximal 96 h after TRITC treatment (Fig. 4*D*). Strikingly fewer $TRITC^+$ LC were isolated from LN of LC/EpCAM-cKO mice at each of the time points examined, with only 25–30% of normal numbers recovered 96 and 120 h after hapten application (Fig. 4*D*).

Exaggeration of Contact Hypersensitivity Responses in LC/EpCAM-cKO Mice. Studies of LC-deficient mice have resulted in new insights into LC function. Several years ago, it was determined that mice that were selectively deficient in epidermal LC exhibited exaggerated, prolonged responses to contact sensitizers (11). We predicted that LC/EpCAM-cKO mice might display a similar phenotype. Thus, WT and EpCAM-cKO mice were treated with 2, 4-dinitrofluorobenzene (DNFB) or vehicle and challenged with DNFB on ear skin 5 d later. The ear-swelling responses that ensued were more than twofold greater in KO mice than in WT mice, and the duration of the response also was prolonged (Fig. 5). These results recapitulate those seen in LC-deficient mice (11).

Characterization of LC Morphology and Motility in Situ. Our results suggested that adhesion of LC and KC might be increased in the absence of EpCAM. If so, increased adhesion could result in morphologic changes in LC or in altered LC motility at baseline or after activation. Confocal immunofluorescence microscopy of LC in LC/EpCAM-cKO skin after staining with anti-MHC Class II and anti–ZO-1 Ab (to delineate LC and tight junctions) revealed that KO LC were larger and had longer, more delicate dendrites than LC in WT skin (Fig. 6*A* and Movies S2 and S3). These features were more obvious in skin that had been treated with TNCB for 18 h (Movies S4 and S5) and in skin explants that had been incubated for 72 h, in which WT LC retracted their dendrites and adopted the polarized morphology typical of migrating cells. EpCAM-deficient LC remained highly dendritic and displayed a morphology that suggested arrested migration (Fig. 6*B*). Assessment of the morphology of unperturbed LC in the vertical (z) dimension indicated that in WT mice LC dendrites abut but do not penetrate tight junctions that form

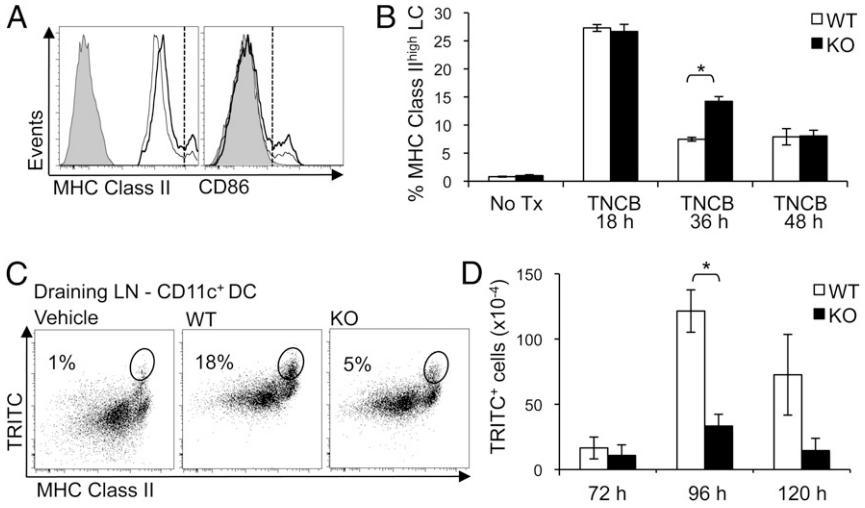

Fig. 4. Defective LC migration in LC/EpCAM-cKO mice in vivo. (*A*) Apparent retention of EpCAM-deficient LC in epidermis after TNCB application. Flow cytometry of CD45$^+$ MHC Class II$^+$ Langerin$^+$ cells in ear epidermal cell suspensions prepared 36 h after 1% TNCB painting revealed a subpopulation of MHC Class II^{high} CD86^{high} activated LC in situ (cells to the right of the vertical dashed line; thick line, KO; thin line, WT; gray line with shading, isotype control). (*B*) Bar graph demonstrating transient retention of activated LC in ear epidermis of LC/EpCAM-cKO (KO) mice 36 h after TNCB painting. Data depicted represent means ± SEM of two or three experiments. $n = 3$ mice per group. *$P < 0.005$. (*C*) Attenuated migration of EpCAM-deficient LC from epidermis to draining LN. Abdominal skin of KO and WT animals was painted with 1% TRITC in dibutyl phthalate:acetone (1:1) or with vehicle, and single-cell suspensions were prepared from skin-draining LN and were analyzed by flow cytometry. Dot plots reveal TRITC$^+$ cells within live-gated CD11c$^+$ cells after 96 h. (*D*) Reduced absolute numbers of TRITC$^+$ cells within live-gated CD11c$^+$ MHC Class II$^+$ Langerin$^+$ CD103$^-$ CD11b$^+$ cells (LC) in LC/EpCAM-cKO mice based on initial cell counts from pooled skin-draining LN at 72, 96, and 120 h after TRITC painting. Data depict means ± SEM from three experiments. $n = 3$ mice per group. *$P < 0.001$.

immediately below the granular layer in epidermis (Fig. 6*C*), as previously reported (9). Interestingly, dendrites of EpCAM-deficient LC appeared to terminate consistently at locations distinctively below that of tight junctions.

To determine if the motility of EpCAM-deficient LC was compromised, we obtained dynamic images of LC in LC/EpCAM-cKO and WT skin. LC/EpCAM-cKO and appropriate control mice were crossed with EYFP reporter mice to generate corresponding LC/EpCAM-cKO and WT mice that expressed EYFP in LC (*Materials and Methods*). LC subsequently were imaged in vivo in real time with a two-photon microscope at baseline (Movie S6) and 18 h after treatment with TNCB (Movie S7). As expected (8), translocation of LC within WT epidermis increased dramatically after TNCB application (Fig. 7*A*). Although TNCB also increased movement of EpCAM-deficient LC within epidermis, TNCB-induced (but not basal) movement of these cells was inhibited by approximately 80% (Fig. 7*A*). EpCAM deletion also altered LC dSEARCH activity, a measure of LC dendrite motility (8). Representative and aggregate data depicted in Fig. 7*B* show that both basal and activation-associated dSEARCH activity was reduced dramatically in EpCAM-deficient LC. These results were confirmed in limited studies involving mice whose LC expressed an MHC Class II-EGFP fusion protein, in which LC dendrites could be imaged in greater detail (Fig. 7*C* and Fig. S4*A*). Interestingly, serial observation of MHC Class II$^{EGFP/+}$ LC/EpCAM-cKO LC 24 h after TNCB-induced activation revealed stationary dendrite tips that appeared to be fixed in the upper epidermis, suggesting enhanced LC–KC adhesion (Fig. 7*D*, Fig. S4*B*, and Movies S8 and S9). Occasionally dendrite tips remained fixed while associated LC bodies moved in the lower epidermis. This phenomenon was not observed in WT LC. These observations of LC dynamics suggest that loss of EpCAM impairs LC disengagement from KC, potentially explaining the elongated LC morphology observed in static images.

Discussion

During the past several years, it has become clear that murine cutaneous DC are heterogeneous (17, 40, 41) and that identifiable DC subsets (including LC) have distinct functions (10–14, 16). Because EpCAM is one of the surface makers that are useful for discriminating LC from other skin DC (6, 17), we were interested in determining if EpCAM plays an important role in LC physiology. Because EpCAM KO mice are nonviable (32), we generated mice with EpCAM-deficient LC by crossing EpCAM$^{fl/fl}$ mice with huLangerinCre^{tg+} mice to address this question. huLangerinCre^{tg+} mice express recombinase in LC but not in other cells (including other Langerin-expressing DC). Thus, the mice that we generated (LC/EpCAM-cKO mice) were expected to have an LC-restricted defect in EpCAM expression.

Initial characterization revealed very efficient inhibition of EpCAM expression by LC in LC/EpCAM-cKO mice. EpCAM expression by KC and intestinal epithelial cells was not affected. Characterization of isolated EpCAM-deficient LC did not reveal abnormalities in cell-surface marker expression, maturation, accessory cell activity, or chemokine-induced migration. In contrast, studies of LC in vivo and skin explants uncovered several differences between control and EpCAM-deficient LC. Although EpCAM-deficient LC could be activated readily, their ability to exit epidermis was attenuated, as reflected in a relative inability of antigen-labeled EpCAM-deficient LC to migrate from epidermis to regional LN, with a resulting increase in contact hypersensitivity. More detailed studies of LC behavior in vivo suggested that loss of EpCAM expression resulted in increased adhesiveness between LC and KC that led to the diminished ability of activated LC to translocate within and out of epidermis as well as to reductions in LC dSEARCH (8) at baseline and after activation.

LC migration from epidermis to LN is a multistep process that requires detachment of LC from KC; up-regulation of relevant chemokine receptors and signaling that results in cytoskeletal rearrangements enabling motility; production of enzymes that mediate paracellular proteolysis that is required for passage of cells through basement membranes and dermal connective tissue; and expression of adhesion molecules that facilate entry into and exit from lymphatic vessels and ultimately localization in the LN paracortex. Previous reports involving KO mice have vali-

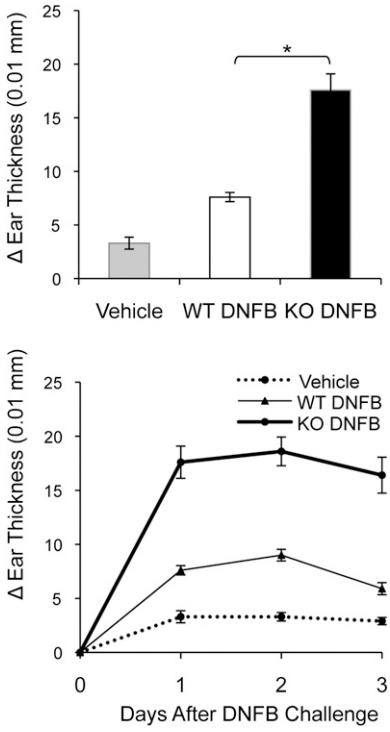

Fig. 5. Functional consequences of the migration defect in LC in LC/EpCAM-cKO mice. Groups of five LC/EpCAM-cKO (KO) and *Cre*-negative littermate control (WT) mice were sensitized with 0.5% DNFB on shaved abdomens on day 0 and were challenged with 0.2% DNFB on ear skin on day 5. Negative control WT mice (Vehicle) were sensitized with vehicle and also were challenged with 0.2% DNFB. (*Upper*) Data represent changes in thicknesses of single ears over baseline at 24 h. (*Lower*) DNFB-induced ear swelling is shown over 3 d in KO (thick line), WT (thin line), and vehicle-alone control mice (thin broken line). Data represent means ± SEM from three experiments. n = 5 mice per group. $^*P < 0.001$.

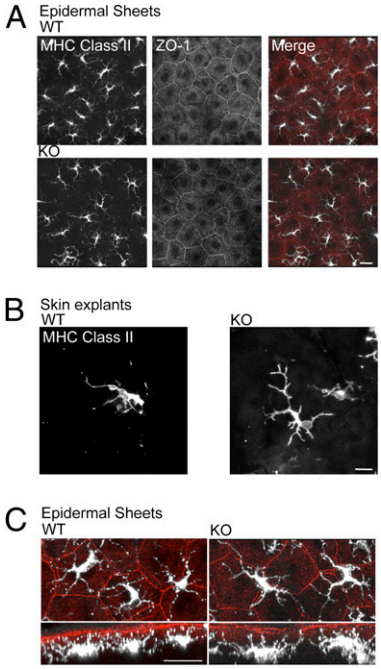

Fig. 6. High-resolution confocal immunfluorescence of LC in situ reveals altered morphology in LC/EpCAM-cKO mice. (*A*) Epidermal sheets were prepared from LC/EpCAM-cKO and WT mice at steady state, stained with anti-MHC Class II mAb and anti-ZO-1 pAb, visualized using confocal microscopy, and are presented as 2D projections of *z*-volumes (WT, z = 35 μm; KO, z = 30 μm). (Scale bar: 15 μm.) (*B*) Confocal images of intraepidermal LC after incubation of skin explants with CCL21 (0.1 μg/mL) for 72 h and staining with anti-MHC Class II mAb. (Scale bar: 10 μm.) (*C*) Composite *en face* images and 90° rotation *z*-stacks of MHC Class II-expressing cells in epidermis at steady state (Scale bar: 10 μm.)

dated the importance of many of these events (42–52), but none have focused on regulation of LC–KC adhesion, and only a few have identified migration abnormalities that do not result from motility defects (46, 47, 51). In addition, no previous studies used mice with LC-restricted defects, and some of the results that have been reported may relate to the behavior of Langerin-expressing dDC in addition to, or even instead of, LC. Studies in the model system that we describe here constitute definitive proof that LC migration is required for LC function in vivo. Because LC dendrite movement (dSEARCH) also is inhibited in LC/EpCAM-cKO mice, it may be possible in future studies to evaluate the physiologic significance of this activity.

The literature regarding EpCAM function in other cells is extensive (for review, see refs. 23 and 36), and it is not easy to synthesize the variety of observations that have been reported into a unified concept. Among the activities attributed to this protein, it has been reported that EpCAM mediates adhesion (25), that it reduces adhesion (26), and that it functions as a signaling molecule (31). Because EpCAM is a molecule that interacts with surrounding cells, it seems likely that context is important. For this reason, in vivo studies of EpCAM function are of particular relevance. To date, only a few studies have assessed endogenous EpCAM function in vivo, and the studies that have been carried out involve seemingly very different contexts [epithelial morphogenesis in zebrafish (53), gastrulation in *Xenopus* (54), placental development (32), and, in this report, LC migration in mice].

Although the contexts explored in these studies are varied, several cross-cutting observations have been made. *EpCAM* zebrafish mutants were identified in a screen for genes that regulate skin development (53). *EpCAM* mutants and morphants exhibited KC abnormalities that resulted in altered epithelial morphogenesis and integrity. These defects were attributed to altered adhesion between superficial and deeper layers of developing epidermis that resulted in morphologic abnormalities [formation of extended apical junctional complexes (tight junctions) and decreased formation of cellular protrusions] and decreased cell migration (epiboly) (53). It has been suggested that EpCAM and E-cadherin are cooperative regulators of this process, but mechanistic details remain to be determined. Depletion of EpCAM in *Xenopus* embryos with morpholinos led to altered gastrulation with ectodermal thickening, and overexpression of EpCAM either in ectoderm or mesoderm caused abnormal cell mixing (54). Structure–function studies indicated that the short cytoplasmic tail that couples EpCAM to the cytoskeleton is both necessary and sufficient to stimulate cell invasion. EpCAM also was demonstrated to act by inhibiting the activity of an atypical PKC that repressed cell mixing when active (54).

Our initial experiments in mice demonstrated that *EpCAM*$^{-/-}$ embryos become nonviable because of placental insufficiency resulting from attenuated development of the labyrinthine layer, a process that involves invasion of fetal elements into the maternal decidua (32). When considered in conjunction with the results of experiments reported here, the data accumulated from studies of EpCAM function in vivo in physiologic contexts suggest that EpCAM is an important regulator of movement of epithelial cells of distinct lineages with respect to each other. Although not yet formally demonstrated in any of these systems, it seems reasonable to hypothesize that EpCAM functions as a modulator of adhesion and that it acts by decreasing (rather than increasing) intercellular adhesion. It is striking that EpCAM and classical

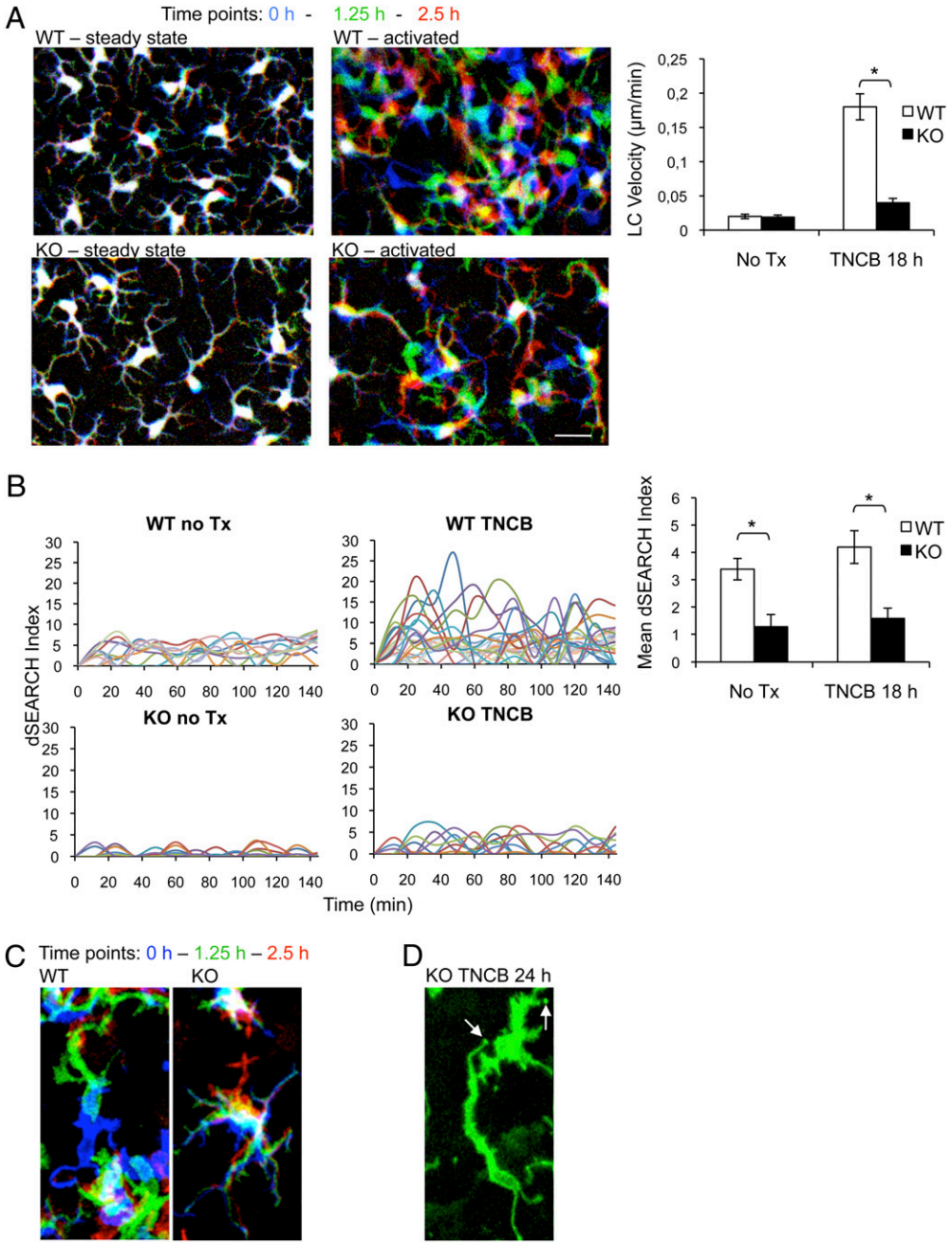

Fig. 7. Decreased LC motility in LC/EpCAM-cKO mice demonstrated via intravital microscopy. (*A*) Two-photon imaging was performed on ears of anesthetized LC/EpCAM-cKO (KO) and WT mice expressing EYFP in LC that were untreated (steady state) or were treated with 1% TNCB 18 h before imaging (activated). Images were acquired every 2 min for 2.5 h, and 3D stacks (steady state, $z = 11$ μm; activated, $z = 18$ μm) were projected into 2D. (*Left*) LC positions are represented with a red/green/blue color code with time 0 in blue, 1:15 h in green, and 2:30 h in red. (Scale bar: 10 μm.) (*Right*) Velocities of cell body movements that were determined for approximately 50 cells per condition and analyzed with ImageJ using the Manual Tracking and Chemotaxis plugins. *$P < 0.01$. (*B*) dSEARCH indices were determined in EYFP-expressing LC in WT and KO mice that had been treated with TCNB 18 h before analysis and were compared with indices in untreated KO and WT mice. (*Left*) Aggregate dendrite position changes of 10 individual LC (indicated in different colors) per group (measured at 12-min intervals over a 144-min observation period. (*Right*) Aggregate mean dSEARCH indices of 50 individual LC per group at steady state or 18 h after ears were painted with 1% TNCB (12-min intervals over 2.5 h). *$P < 0.0001$. Data represent means ± SEM. (*C*) Cell body displacement of MHC Class II-EGFP–labeled LC 18 h after TNCB painting ($z = 18$ μm, projected into 2D). Color coding is as in *A*. (*D*) Immotile dendrite tips (arrows) of MHC Class II-EGFP–expressing, EpCAM-deficient LC 24 h after TNCB painting ($z = 18$ μm, projected into 2D).

cadherins (especially E-cadherin) are coexpressed in tissues/cells in which EpCAM has been shown to have physiologic roles, and it has been reported previously that EpCAM can modulate cadherin-mediated adhesion (26). At present, it is not clear if EpCAM modulates cadherin function, and precise mechanisms by which this modulation might be accomplished have not been delineated. It also is not obvious that the outside–in signaling activity that has been attributed to EpCAM (31) is linked to the changes in cell behavior that have been observed in vivo.

EpCAM has been studied most extensively in cancer. Although there are controversies, EpCAM may facilitate cancer cell invasion and metastasis, and it has been suggested that

EpCAM expression in tumors indicates poor prognosis (23, 29, 36). This viewpoint is attractive, because it is consistent with the suggestion that EpCAM is a negative regulator of adhesion between epithelial cells. EpCAM expression by tumor cells might promote detachment of tumor cells from normal epithelial cells (or metastatic cells from malignant cells in primary tumors), just as EpCAM may faciliate detachment of LC from KC before movement from epithelia to LN. Elucidation of the signaling pathways that are involved in regulation of intercellular adhesion by EpCAM through studies of the conditional KO mice that we have generated and strains that may be generated in the future may lead to identification of new targets that are relevant for development of cancer therapeutics and/or immunomodulators.

Materials and Methods

Mice. Mice generated at the National Cancer Institute are described below and in *SI Materials and Methods*. huLangerinCre^{tg+} mice were provided by Daniel Kaplan (University of Minnesota, Minneapolis, MN). ROSA26 stop$^{fl/fl}$EYFP reporter mice (55) were purchased from Jackson Laboratories, and MHCII$^{EGFP/+}$ knockin reporter mice (56) were obtained from Taconic. All mice were bred and housed in a pathogen-free environment and were used in experiments at the National Institutes of Health in accordance with institutional guidelines.

Preparation of Epidermal Sheets and Single-Cell Suspensions. Epidermal sheets, epidermal cell suspensions, and LN cell suspensions were prepared as described in *SI Materials and Methods*.

Antibodies and Flow Cytometry. The antibodies used for these studies are detailed in *SI Materials and Methods*. Data were collected with a LSRII flow cytometer (BD) and analyzed with FlowJo software (Treestar). Nonviable cells were excluded after 7-AAD (BD) staining, unless cells had been fixed and permeabilized.

Mixed Epidermal Cell–Allogeneic T-Cell Reactions. Primary mixed epidermal cell–allogeneic T-cell reactions were carried out as decribed in *SI Materials and Methods*.

Assessment of LC Emigration Using Skin Explants. Skin explants were prepared as previously described (37). Ears were divided into dorsal and ventral halves, cartilage and s.c. tissue was removed, and skin was floated on RPMI medium 1640 (Invitrogen) containing 10% (vol/vol) heat-inactivated FBS (HyClone), 2 mM glutamine, 0.1 mM nonessential amino acids, 10 mM Hepes, 1% antibiotic/antimycotic (all from Invitrogen), 50 μM 2-mercaptoethanol (Sigma), and 0.1 μg/mL CC chemokine ligand 21 (CCL21) (R&D Systems). Explants were cultured for 72 h. DC that accumulated in the medium were enumerated using Trypan blue (Invitrogen) and a hemocytometer (Neubauer) and were characterized via flow cytometry. Absolute numbers of LC (MHC Class II^{high} Langerin^{+} CD103^{-}) and dDC (MHC Class II^{high} Langerin^{+} CD103^{+}) that migrated from explants were calculated. Epidermal and dermal sheets were prepared from skin explants as described below.

Assessment of LC Chemotaxis in Vitro. LC chemotaxis in collagen gels was assessed as previously described (39). Epidermal cell suspensions were cultured in complete RPMI medium for 3 d, enriched for leukocytes using Lympholyte-M density gradients (Cedarlane), added to soluble bovine collagen type I (PureCol; Advanced BioMatrix) in Eagle's minimal essential medium at room temperature, and warmed to 37 °C after introduction into specially prepared migration chambers (39). Polymerized gels were overlaid with culture medium containing CCL19 (0.5 μg/mL), and cells were imaged using a Zeiss AxioObserver Z1 inverted microscope equipped with a heated stage, AxioVision (v.4.8) software, and either 10× (Plan-Apochromat N.A. 0.45) or 20× (Plan-Apochromat 0.8) objective lenses, with or without the 1.6× Optovar. Images of migrating LC were taken at 20-s intervals over 3-h periods, and velocities were quantified with ImageJ software (National Institues of Health) using the Manual Tracking and Chemotaxis tools.

Application of Haptens and Measurement of Contact Hypersensitivity Reactions. LC activation in situ was achieved by applying 10 μL of 1% TNCB in acetone:olive oil (4:1) to dorsal and ventral ear skin. Assessments were performed at the indicated times. In some experiments, LC were activated and labeled in situ using TRITC (Invitrogen) prepared as a 100-mg/mL (10% wt/vol) stock solution in DMSO and diluted to 1% in acetone and dibutyl phthalate (1:1) before application (100 μL) onto clipped abdominal skin. Contact hypersensivity reactions to DNFB were elicited and quantified as described in *SI Materials and Methods*.

Immunofluorescence Microscopy of Epidermal Sheets. Epidermal sheets were prepared from ear skin and incubated in 3% (wt/vol) dry milk-PBS (Bio-Rad) and 5 μg/mL rat anti-CD16/32 mAb (BD) for 1 h at room temperature to minimize nonspecific staining before incubation with fluorochrome-labeled mAb (5 μg/mL) for 1 h at room temperature or overnight at 4 °C. Conventional immunofluorescence microscopy was performed using an AxioImager A1 (Carl Zeiss Microimaging). Intensities of digital images in experimental and control specimens were adjusted within the linear range with Zeiss Axiovison software (all Carl Zeiss) and ImageJ. LC and dendritic epidermal T-cell (DETC) densities were determined by counting five random fields per animal at 200× final magnification. Confocal microscopy was performed with an inverted LSM710 confocal microscope (Carl Zeiss Microimaging) equipped with a 63×/NA 1.40 oil Plan-Apochromat objective using 0.3-μm optical slices. 3D image stacks were reconstructed and animated with Imaris software (Bitplane).

Two-Photon Intravital Skin Imaging and Image Analysis. To visualize LC in intravital studies, LC/EpCAM-cKO mice were crossed to Rosa26 stop$^{fl/fl}$ EYFP mice, resulting in selective EYFP expression in LC, and to MHCII$^{EGFP/+}$ knockin mice to achieve low EGFP expression in dDC and high EGFP expression in mature LC. This third strain was used in a limited number of confirmatory experiments and allowed visualization of LC dendrites with higher resolution. Two-photon intravital skin imaging was performed as previously described (57). Mice were anesthetized using isoflurane (Baxter), and the ventral sides of ear pinnae were fixed to coverslips at the bottom of the imaging platform with tape strips. Images were acquired using an inverted LSM 510 NLO multiphoton microscope (Carl Zeiss Microimaging) enclosed in a custom environmental chamber with heated (32 °C) air. Images were acquired using a 25×/0.8 NA Plan-Apochromat objective (Carl Zeiss Imaging) with glycerol as the immersion medium. Fluorescence excitation was accomplished with a Chamelon XR Ti:Sapphire laser (Coherent) tuned to 920 nm for EGFP and to 940 nm for EYFP excitation. For 4D data sets, 3D stacks were captured every 2 min.

Raw imaging data were processed with Imaris (Bitplane) using a Gaussian filter for noise reduction. All images and movies are displayed as 2D maximum intensity projections unless otherwise stated. dSEARCH indices were calculated using an approach analogous to that of Nishibu and coworkers (8) Briefly, position changes of all dendrite tips corresponding to individual LC were tracked over the observation period, quantified using ImageJ and the Manual Tracking and Chemotaxis plugins, and are expressed on a per cell basis and as aggregated results for the numbers of LC indicated.

Statistical Analysis. Statistical significance was determined using Prism5 for Mac (GraphPad Software). The Student's *t* test was used after confirming that all data fulfilled the criteria of normal distribution and equal variance. $P < 0.05$ was considered statistically significant.

ACKNOWLEDGMENTS. We thank Drs. William Telford and Michael Kruhlak for their advice and assistance with flow cytometry and conventional microscopy; Joshua Drago, Mallorie Heneghan, and Olga Milgrom for mouse husbandry and genotyping; Jay Linton, Michael Lu, Dr. Chuanjin Wu, and Dr. Sei-ichiro Motegi for advice and assistance with experimental procedures; and Dr. Stephen I. Katz for helpful discussions. This work was supported by the Intramural Research Program, Center for Cancer Research, National Cancer Institute, and the National Institues of Allergy and Infectious Diseases, National Institutes of Health, by National Institutes of Health Grant R01-AR056632 (to D.H.K.), and an International Human Frontier Science Program fellowship grant (to T.L.).

1. Birbeck MS, Breathnach AS, Everall JD (1961) An electron microscope study of basal melanocytes and high-level clear cells (Langerhans cells) in vitiligo. *J Invest Dermatol* 37:51–63.
2. Borkowski TA, Letterio JJ, Farr AG, Udey MC (1996) A role for endogenous transforming growth factor beta 1 in Langerhans cell biology: The skin of transforming growth factor beta 1 null mice is devoid of epidermal Langerhans cells. *J Exp Med* 184:2417–2422.
3. Merad M, Ginhoux F, Collin M (2008) Origin, homeostasis and function of Langerhans cells and other langerin-expressing dendritic cells. *Nat Rev Immunol* 8: 935–947.
4. Valladeau J, et al. (2000) Langerin, a novel C-type lectin specific to Langerhans cells, is an endocytic receptor that induces the formation of Birbeck granules. *Immunity* 12: 71–81.

5. Tang A, Amagai M, Granger LG, Stanley JR, Udey MC (1993) Adhesion of epidermal Langerhans cells to keratinocytes mediated by E-cadherin. *Nature* 361:82–85.
6. Borkowski TA, Nelson AJ, Farr AG, Udey MC (1996) Expression of gp40, the murine homologue of human epithelial cell adhesion molecule (Ep-CAM), by murine dendritic cells. *Eur J Immunol* 26:110–114.
7. Eisenwort G, et al. (2011) Identification of TROP2 (TACSTD2), an EpCAM-like molecule, as a specific marker for TGF-β1-dependent human epidermal Langerhans cells. *J Invest Dermatol* 131:2049–2057.
8. Nishibu A, et al. (2006) Behavioral responses of epidermal Langerhans cells in situ to local pathological stimuli. *J Invest Dermatol* 126:787–796.
9. Kubo A, Nagao K, Yokouchi M, Sasaki H, Amagai M (2009) External antigen uptake by Langerhans cells with reorganization of epidermal tight junction barriers. *J Exp Med* 206:2937–2946.
10. Bennett CL, et al. (2005) Inducible ablation of mouse Langerhans cells diminishes but fails to abrogate contact hypersensitivity. *J Cell Biol* 169:569–576.
11. Kaplan DH, Jenison MC, Saeland S, Shlomchik WD, Shlomchik MJ (2005) Epidermal langerhans cell-deficient mice develop enhanced contact hypersensitivity. *Immunity* 23:611–620.
12. Kissenpfennig A, et al. (2005) Dynamics and function of Langerhans cells in vivo: Dermal dendritic cells colonize lymph node areas distinct from slower migrating Langerhans cells. *Immunity* 22:643–654.
13. Aebischer T, et al. (2005) A critical role for lipophosphoglycan in proinflammatory responses of dendritic cells to Leishmania mexicana. *Eur J Immunol* 35:476–486.
14. Allan RS, et al. (2003) Epidermal viral immunity induced by CD8alpha+ dendritic cells but not by Langerhans cells. *Science* 301:1925–1928.
15. Igyarto BZ, et al. (2009) Langerhans cells suppress contact hypersensitivity responses via cognate CD4 interaction and langerhans cell-derived IL-10. *J Immunol* 183: 5085–5093.
16. Kautz-Neu K, et al. (2011) Langerhans cells are negative regulators of the anti-Leishmania response. *J Exp Med* 208:885–891.
17. Nagao K, et al. (2009) Murine epidermal Langerhans cells and langerin-expressing dermal dendritic cells are unrelated and exhibit distinct functions. *Proc Natl Acad Sci USA* 106:3312–3317.
18. Igyártó BZ, et al. (2011) Skin-resident murine dendritic cell subsets promote distinct and opposing antigen-specific T helper cell responses. *Immunity* 35:260–272.
19. Takeichi M (1990) Cadherins: A molecular family important in selective cell-cell adhesion. *Annu Rev Biochem* 59:237–252.
20. Schwarzenberger K, Udey MC (1996) Contact allergens and epidermal proinflammatory cytokines modulate Langerhans cell E-cadherin expression in situ. *J Invest Dermatol* 106:553–558.
21. Jiang A, et al. (2007) Disruption of E-cadherin-mediated adhesion induces a functionally distinct pathway of dendritic cell maturation. *Immunity* 27:610–624.
22. Riedl E, et al. (2000) Ligation of E-cadherin on in vitro-generated immature Langerhans-type dendritic cells inhibits their maturation. *Blood* 96:4276–4284.
23. Trzpis M, McLaughlin PM, de Leij LM, Harmsen MC (2007) Epithelial cell adhesion molecule: More than a carcinoma marker and adhesion molecule. *Am J Pathol* 171: 386–395.
24. Schiechl H, Dohr G (1987) Immunohistochemical studies of the distribution of a basolateral-membrane protein in intestinal epithelial cells (GZ1-Ag) in rats using monoclonal antibodies. *Histochemistry* 87:491–498.
25. Litvinov SV, Velders MP, Bakker HA, Fleuren GJ, Warnaar SO (1994) Ep-CAM: A human epithelial antigen is a homophilic cell-cell adhesion molecule. *J Cell Biol* 125:437–446.
26. Litvinov SV, et al. (1997) Epithelial cell adhesion molecule (Ep-CAM) modulates cell-cell interactions mediated by classic cadherins. *J Cell Biol* 139:1337–1348.
27. Sears HF, et al. (1982) Phase-I clinical trial of monoclonal antibody in treatment of gastrointestinal tumours. *Lancet* 1:762–765.
28. Baeuerle PA, Gires O (2007) EpCAM (CD326) finding its role in cancer. *Br J Cancer* 96: 417–423.
29. van der Gun BT, et al. (2010) EpCAM in carcinogenesis: The good, the bad or the ugly. *Carcinogenesis* 31:1913–1921.
30. Gires O, Klein CA, Baeuerle PA (2009) On the abundance of EpCAM on cancer stem cells. *Nat Rev Cancer* 9:143–author reply 143.
31. Maetzel D, et al. (2009) Nuclear signalling by tumour-associated antigen EpCAM. *Nat Cell Biol* 11:162–171.
32. Nagao K, et al. (2009) Abnormal placental development and early embryonic lethality in EpCAM-null mice. *PLoS ONE* 4:e8543.
33. Stryke D, et al. (2003) BayGenomics: A resource of insertional mutations in mouse embryonic stem cells. *Nucleic Acids Res* 31:278–281.
34. Copeland NG, Jenkins NA, Court DL (2001) Recombineering: A powerful new tool for mouse functional genomics. *Nat Rev Genet* 2:769–779.
35. Wu Y, Wang C, Sun H, LeRoith D, Yakar S (2009) High-efficient FLPo deleter mice in C57BL/6J background. *PLoS ONE* 4:e8054.
36. Trzpis M, Bremer E, McLaughlin PM, de Leij LF, Harmsen MC (2008) EpCAM in morphogenesis. *Front Biosci* 13:5050–5055.
37. Larsen CP, Morris PJ, Austyn JM (1990) Migration of dendritic leukocytes from cardiac allografts into host spleens. A novel pathway for initiation of rejection. *J Exp Med* 171:307–314.
38. Lukas M, et al. (1996) Human cutaneous dendritic cells migrate through dermal lymphatic vessels in a skin organ culture model. *J Invest Dermatol* 106:1293–1299.
39. Sixt M, Lämmermann T (2011) In vitro analysis of chemotactic leukocyte migration in 3D environments. *Methods Mol Biol* 769:149–165.
40. Bursch LS, et al. (2007) Identification of a novel population of Langerin+ dendritic cells. *J Exp Med* 204:3147–3156.
41. Henri S, et al. (2010) CD207+ CD103+ dermal dendritic cells cross-present keratinocyte-derived antigens irrespective of the presence of Langerhans cells. *J Exp Med* 207:189–206.
42. de Noronha S, et al. (2005) Impaired dendritic-cell homing in vivo in the absence of Wiskott-Aldrich syndrome protein. *Blood* 105:1590–1597.
43. Del Prete A, et al. (2004) Defective dendritic cell migration and activation of adaptive immunity in PI3Kgamma-deficient mice. *EMBO J* 23:3505–3515.
44. Fukunaga A, et al. (2006) Src homology 2 domain-containing protein tyrosine phosphatase substrate 1 regulates the induction of Langerhans cell maturation. *Eur J Immunol* 36:3216–3226.
45. Kabashima K, et al. (2003) Prostaglandin E2-EP4 signaling initiates skin immune responses by promoting migration and maturation of Langerhans cells. *Nat Med* 9: 744–749.
46. Maddaluno L, et al. (2009) The adhesion molecule L1 regulates transendothelial migration and trafficking of dendritic cells. *J Exp Med* 206:623–635.
47. Ratzinger G, et al. (2002) Matrix metalloproteinases 9 and 2 are necessary for the migration of Langerhans cells and dermal dendritic cells from human and murine skin. *J Immunol* 168:4361–4371.
48. Rubic T, et al. (2008) Triggering the succinate receptor GPR91 on dendritic cells enhances immunity. *Nat Immunol* 9:1261–1269.
49. Sangaletti S, et al. (2005) Accelerated dendritic-cell migration and T-cell priming in SPARC-deficient mice. *J Cell Sci* 118:3685–3694.
50. Sato N, et al. (2000) CC chemokine receptor (CCR)2 is required for langerhans cell migration and localization of T helper cell type 1 (Th1)-inducing dendritic cells. Absence of CCR2 shifts the Leishmania major-resistant phenotype to a susceptible state dominated by Th2 cytokines, b cell outgrowth, and sustained neutrophilic inflammation. *J Exp Med* 192:205–218.
51. Wang M, et al. (1999) Matrix metalloproteinase deficiencies affect contact hypersensitivity: Stromelysin-1 deficiency prevents the response and gelatinase B deficiency prolongs the response. *Proc Natl Acad Sci USA* 96:6885–6889.
52. Yamakita Y, et al. (2011) Fascin1 promotes cell migration of mature dendritic cells. *J Immunol* 186:2850–2859.
53. Slanchev K, et al. (2009) The epithelial cell adhesion molecule EpCAM is required for epithelial morphogenesis and integrity during zebrafish epiboly and skin development. *PLoS Genet* 5:e1000563.
54. Maghzal N, Vogt E, Reintsch W, Fraser JS, Fagotto F (2010) The tumor-associated EpCAM regulates morphogenetic movements through intracellular signaling. *J Cell Biol* 191:645–659.
55. Srinivas S, et al. (2001) Cre reporter strains produced by targeted insertion of EYFP and ECFP into the ROSA26 locus. *BMC Dev Biol* 1:4.
56. Boes M, et al. (2002) T-cell engagement of dendritic cells rapidly rearranges MHC class II transport. *Nature* 418:983–988.
57. Peters NC, et al. (2008) In vivo imaging reveals an essential role for neutrophils in leishmaniasis transmitted by sand flies. *Science* 321:970–974.

Correction

IMMUNOLOGY

Correction for "Cancer-associated epithelial cell adhesion molecule (EpCAM; CD326) enables epidermal Langerhans cell motility and migration in vivo," by Maria R. Gaiser, Tim Lämmermann, Xu Feng, Botond Z. Igyarto, Daniel H. Kaplan, Lino Tessarollo, Ronald N. Germain, and Mark C. Udey, which appeared in issue 15, April 10, 2012, of *Proc Natl Acad Sci USA* (109:E889–E897; first published March 12, 2012; 10.1073/pnas.1117674109).

The authors note that Fig. 1 and its corresponding legend appeared incorrectly. The corrected figure and its corrected legend appear below. This error does not affect the conclusions of the article.

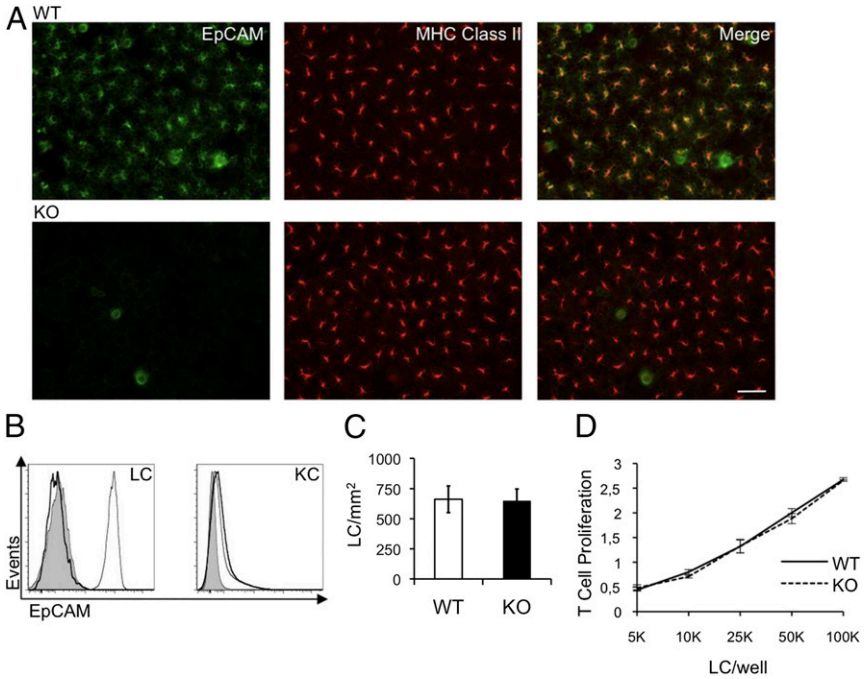

Fig. 1. Characterization of EpCAM-deficient LC in LC/EpCAM-cKO mice. (*A*) Demonstration in situ via immunofluorescence microscopy of EpCAM deletion in LC in LC/EpCAM-cKO mice. Epidermal sheets from LC/EpCAM-cKO (KO) and *Cre*-negative (WT) animals were stained with anti-EpCAM and anti-MHC Class II mAb and visualized using immunofluorescence microscopy. (Scale bar: 50 μm.) Note residual EpCAM expression in hair follicles in WT and KO mice. (*B*) Demonstration via flow cytometry of EpCAM deletion in LC in LC/EpCAM-cKO mice. Flow cytometric analysis of $CD45^+$ MHC Class II^+ $Langerin^+$ cells (LC) and $CD45^-$ MHC Class II^- cells (KC) in epidermal cell suspensions from LC/EpCAM-cKO (KO) and WT animals. $n = 3$ mice per group in three experiments; thick line, KO; WT, thin line, WT; gray line with shading, isotype control. EpCAM expression levels are depicted as geometric mean fluorescence intensities (MFI). (*C*) LC densities in LC/EpCAM-cKO mice. LC were enumerated by counting MHC Class II^+ cells in epidermal sheets from KO and WT mice (10 random fields per mouse, 3–4 mice per group). Data presented are representative of three experiments. (*D*) T-cell–stimulatory activity of EpCAM-deficient LC. Epidermal cells from KO and WT mice were cocultured with MHC-mismatched (BALB/c) naive T cells ($n = 3$ mice per group in three experiments using triplicate measurements in each experiment). Numbers of LC per well were determined using flow cytometry to assess LC frequencies in epidermal single-cell suspensions. T-cell proliferation was measured by quantifying cleavage of WST-1 using a spectrophotometric assay.

www.pnas.org/cgi/doi/10.1073/pnas.1604056113